water

MDPI

Article

Key Techniques for the Ultra-Deep Large Flood Diversion Pipeline: A Case Study of Jinshui River Flood Diversion Project in Zhengzhou

Hao Zhou [1,2], Haitao Wang [3], Sheng Huang [1,2,*], Baosong Ma [1,2] and Peng Ma [1]

[1] School of Civil Engineering, Sun Yat-sen University, Guangzhou 510275, China; zhouh253@mail2.sysu.edu.cn (H.Z.)
[2] State Key Laboratory for Tunnel Engineering, Guangzhou 510275, China
[3] Zhengzhou Zhengfa Water Conservancy Engineering Co., Ltd., Zhengzhou 450006, China
* Correspondence: huangsh98@mail.sysu.edu.cn

Abstract: The implementation of large-diameter flood diversion pipelines in urban areas serves as an effective strategy to address urban waterlogging issues, which can enhance the resilience of cities to a certain extent against extreme precipitation events. This case study delineates the Zhengzhou Jinshui River flood diversion project, which employs the ultra-large-buried jacking prestressed concrete cylinder pipe (JPCCP), offering a summary and analysis of the pipe design and construction technologies employed in the JPCCP project within collapsible loess stratum, and the study also analyzes the pull-back scheme of the incident involving the front-end sinking of the machine head. Through on-site monitoring experiments, the variation patterns of contact pressure and slurry pressure of large-diameter JPCCPs were analyzed. The results demonstrate that the trends in contact pressure and slurry pressure exhibit a general consistency. During the jacking process, the pressure around the pipe can be categorized into three distinct phases based on grouting frequency or pressure, with notable variations in the pipe–soil–slurry contact state. The difference between the contact pressure and slurry pressure (termed as effective soil pressure) serves as a more accurate method for determining the pipe's operational state. Moreover, the effective earth pressure at the pipe top demonstrates a higher degree of consistency with the calculation results prescribed by the standards ATV A161 and ASCE 27.

Keywords: flood diversion pipeline; collapsible loess stratum; JPCCP; pipe jacking; pipe–soil–slurry interaction

check for updates

Academic Editor: David Post

Received: 21 November 2024
Revised: 13 December 2024
Accepted: 21 December 2024
Published: 24 December 2024

Citation: Zhou, H.; Wang, H.; Huang, S.; Ma, B.; Ma, P. Key Techniques for the Ultra-Deep Large Flood Diversion Pipeline: A Case Study of Jinshui River Flood Diversion Project in Zhengzhou. *Water* **2025**, *17*, 13. https://doi.org/10.3390/w17010013

Copyright: © 2024 by the authors. Licensee MDPI, Basel, Switzerland. This article is an open access article distributed under the terms and conditions of the Creative Commons Attribution (CC BY) license (https://creativecommons.org/licenses/by/4.0/).

1. Introduction

Climate change has led to frequent extreme precipitation events. To address urban waterlogging stemming from extreme precipitation, China is actively promoting the construction of flood-diversion and water-logging drainage pipelines in cities, thereby enhancing urban resilience to some extent [1]. Due to the development of technology, there are many pipeline-laying methods at present. Conversely, the pipe jacking method offers notable benefits encompassing low environmental impact, enhanced safety and reliability, and robust adaptability to varying stratum conditions [2]. So, the pipe jacking method is especially well-suited for the construction of long-distance, large-scale, and deep-buried flood-diversion pipelines in water conservancy projects [3].

Currently, pipe jacking construction commonly utilizes various materials including concrete pipe, steel pipe, nodular cast iron pipe, and fiberglass reinforced plastic sand pipe.

However, there are more and more projects using jacking prestressed concrete cylinder pipe (JPCCP) as the jacking pipe. In contrast, JPCCP pipe exhibits superior strength, capable of withstanding higher external loads and internal water pressure [4,5]. Moreover, it offers excellent pressure resistance, impermeability, and corrosion resistance, thereby making it highly favored in water conservancy projects [6,7]. The design and construction of ultra-large diameter JPCCP differ from those of traditional reinforced concrete pipes or steel pipes, and there is limited research in this area. Some scholars have conducted axial jacking experiments on large-diameter JPCCP, assessing the annular structural stress characteristics and safety performance of JPCCP under varied working conditions [8]. In terms of field tests, Zhang et al. [6] and Shen et al. [7] observed that the concrete core exhibited the capacity to withstand substantial circumferential tensile stress, emphasizing the significant impact of wire prestress loss on the bearing capacity of JPCCP. Zhou et al. [9,10] observed that the prestressing wires at different positions exhibited both tension and relaxation phenomena. Notably, the deformation of the wires in pipe's central section was greater that at the bell–spigot end. Under the combined effects of non-full-section eccentric compression and jacking force transmission, the transmission of jacking force within the exterior-reinforced concrete was more evident.

Furthermore, the pipe-jacking project falls under the category of underground space engineering, where the geotechnical properties and grouting processes are crucial to the interaction between the pipe and the surrounding soil. While there are numerous engineering cases of large-diameter pipe-jacking in general strata, significant challenges arise in collapsible soil. Due to the loose soil in the collapsible loess stratum, the stability of the excavation face of the pipe jacking, and the flexible connection of the pipes, the anti-seepage and pressure-holding of the pipe are easily affected by the disturbance soaking, which poses a challenge to the smooth construction of the ultra-large pipe jacking. Khodabandeh et al. [11] explored the feasibility and effectiveness of various stabilizing materials, including nano-materials, fibers, polymers, industrial waste, and microbes, for improving collapsible soil. However, due to the extensive soil excavation induced by the pipe-jacking process, slurry remains the predominant method for soil lubrication and support in practical engineering applications [12].

The interaction between the pipe and surrounding soil directly affects the distribution of the load on pipes. Numerous engineering experiments have shown that the contact pressure of the pipe-jacking during construction is primarily composed of water–soil pressure and slurry pressure, with the latter playing a controlling role and influencing the interaction between the pipe and soil contact states [12]. Liu et al. [13] proposed that, depending on the volume of grouting, grouting pressure, and grout density, four distinct pipe–grout–soil interaction modes exist. Under conditions of adequate grouting, the contact mode of the pipe can be determined based on the resultant force of the pipe. Liu et al. [14] designed four interface contact conditions and conducted indoor direct shear tests at five different normal stress levels. Based on macroscopic and microscopic images observed during the tests, the lubrication mechanism of the lubricant was analyzed.

The Jinshui River Flood Diversion Project in Zhengzhou is one of the JPCCP projects with the largest diameter, the longest single jacking, and the largest buried depth in China. The pipeline primarily traverses collapsible loess strata, presenting significant engineering challenges during the pipe-jacking construction. This case study recognizes the complexity of the flood diversion project construction and provides a comprehensive summary and analysis of the key technologies involved in JPCCP design and construction. Additionally, it evaluates the effectiveness of emergency response measures and construction control strategies. Finally, field tests were conducted to monitor the contact and slurry pressures throughout the entire pipe-jacking construction cycle, the variations in the surrounding

pipe pressure were analyzed, and the calculation method for the pipe–soil pressure in the loess strata was discussed.

2. Engineering Background

2.1. Project Overview

Zhengzhou City lies within the transitional zone connecting the second and third levels of China's geomorphic terrace, featuring a terrain inclined from the southwest to the northeast. The topographical and hydrological characteristics of Zhengzhou City are visually depicted in Figure 1. Serving as one of the urban inland rivers, the Jinshui River courses through the main urban area, marked by numerous waterlogging points along its course, presenting a high risk of flooding. From 17 to 23 July 2021, Henan Province experienced the impact of abnormal atmospheric circulation and typhoons, leading to an unprecedented and rare extreme precipitation event. Specifically, Zhengzhou City, the provincial capital of Henan, incurred significant human casualties and economic losses during this period [15].

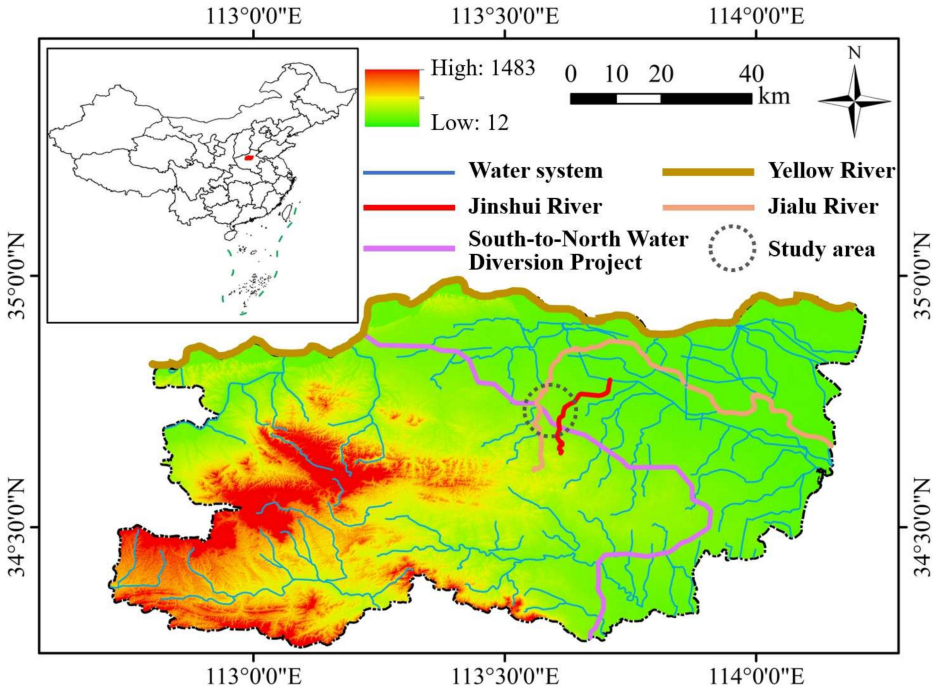


Figure 1. The topographical and hydrological characteristics of Zhengzhou City.

The Jinshui River Flood Diversion Project, pivotal for post-disaster reconstruction, aims to connect the Jinshui River and the Jialu River, and its primary objective is to elevate urban flood control standards, ensuring a 200-year level of protection in the main urban area. Figure 2 illustrates the plan of the study area. The comprehensive investment in the flood diversion project amounts to 1.23 billion yuan, and the principal components of this undertaking encompass both pipe-jacking projects and open caisson projects; the total length of the entire pipeline extends over 5.44 km, featuring a designed conveyance capacity of 75 m^3/s. Along the flood diversion pipeline, 15 circular caissons are arranged, incorporating eight launch shafts and seven receiving shafts, and the design parameters of the caissons and pipe-jacking intervals are detailed in Table 1. The diameter and depth of the caissons represent an uncommon scale in China, and the pipeline employs the parallel laying of double-row DN4000 JPCCP, with a 6 m separation between the two pipes. The JPCCP has an inner diameter of 4 m, an outer diameter of 4.8 m, and a weight of 45 t. The flood diversion pipeline alleviates Jinshui River waterlogging within the city, beginning at

the head end from the 1# (R1) shaft and channeling it to the Jialu River through the 15# (L8) shaft at the terminus. The buried depth along the pipeline ranges from 7 m at the shallowest to 36 m at the deepest, rendering the construction process exceedingly challenging [9,10].

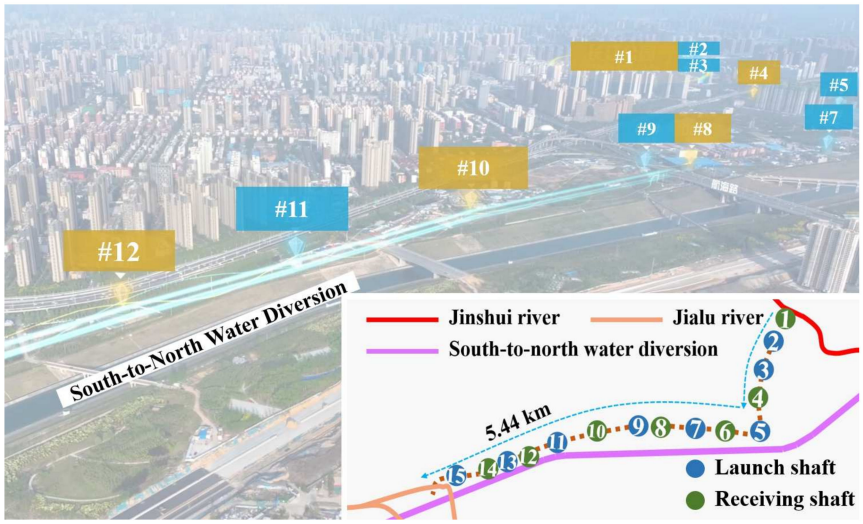


Figure 2. The layout of the Jinshui River Flood Diversion Pipeline in the study area.

Table 1. The design parameters of the caissons and pipe-jacking intervals.

Working Shaft	Diameter of Shaft (m)	Depth of Shaft (m)	Jacking Distance (m)
1# (R1)	22.60	15.98	262.41
2# (L1)	21.60	18.68	164.7
3# (L2)	21.60	16.09	494.49
4# (R2)	20.00	23.67	398.87
5# (L3)	34.00	29.32	406.32
6# (R3)	20.00	31.45	506.75
7# (L4)	21.60	33.83	516.88
8# (R4)	20.00	36.70	129.24
9# (L5)	21.60	37.59	659.33
10# (R5)	20.00	35.12	437.08
11# (L6)	21.60	32.54	357.32
12# (R6)	20.00	28.85	494.45
13# (L7)	21.60	31.18	91.14
14# (R7)	26.00	29.76	148.27
15# (L8)	26.00	29.85	337.45

Note: L is the launch shaft and R is the receiving shaft.

2.2. Geological Conditions in the Study Area

The geological composition of the engineering site from top to bottom, as determined by the survey, comprises ① Artificial fill, ② Light silty loam-like loess, and ③ Medium silty loam-like loess, and the pipe mainly passes through the ② Light silty loam-like loess layer. The geological profile, encompassing 15 working shafts and pipe-jacking intervals, is elucidated in Figure 3, while Table 2 comprehensively details the recommended physical parameters of the stratum. Calculated according to GB50025-2018 [16], the collapsible depth at the adjacent site is 7 m, with a self-weight collapsible amount of 78.6 mm and a total collapsible amount of 319.7 mm. This classification designates the site as self-weight collapsible, categorized as Level II (Medium), with the initial collapse pressure ranging from 91 to 150 kPa.

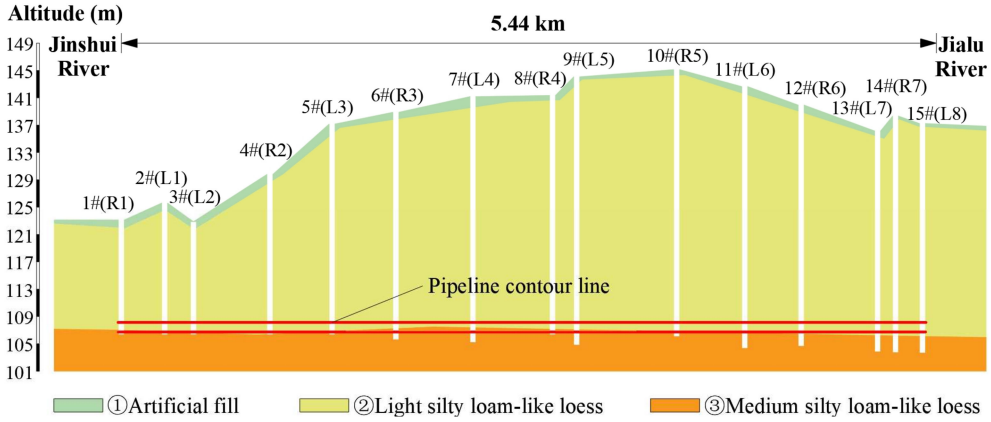


Figure 3. Longitudinal engineering geological profile.

Table 2. The recommended physical parameters of the stratum.

Soil Layer	Dry Density ($g \cdot cm^{-3}$)	Cohesion (kPa)	Internal Friction Angle (°)	Compression Modulus (Mpa)
① Artificial fill	-	-	-	-
② Light silty loam-like loess	1.60	11.4	17.8	8.3
③ Medium silty loam-like loess	1.64	18.2	11.9	7.4

2.3. Engineering Difficulties

The flood diversion pipeline project is situated within the urban area of Zhengzhou; thus, addressing how to expedite the construction within a confined timeframe stands as a critical challenge for this project. The particular challenges encountered in the project are as follows:

(1) As a systematic project of multi-process coordination and intersection, the construction of ultra-deep large caissons and long-distance pipe jacking will cause problems such as disconnection between construction progress and plan, conflict over process resources, and increases in the additional cost. Consequently, a pivotal challenge in construction lies in determining construction strategies to optimize efficiency during the period, thereby enhancing overall effectiveness.

(2) Collapsible loess exhibits characteristics of a loose structure, limited adhesion between soil particles, and the presence of a small number of calcareous nodules. The geological conditions necessitate elevated standards for the rotary cutting performance of the cutterhead. During the soil-cutting process by the cutterhead, mud infiltration can lead to the 'mud cake' phenomenon, and ongoing excavation may obstruct the soil outlet, thereby impacting the cutting and slag discharge efficiency. Consequently, there is a need for a rational design of both the cutterhead and the slurry cabin.

(3) Long-distance, large-diameter pipe-jacking projects are inherently confronted with a range of challenges, including the substantial weight of the cutterhead and pipes, heightened sensitivity to stratum variations, difficulties in controlling pipe alignment, and stringent demands for jacking force. During the project, an incident involving the front-end sinking of the machine head occurred, and the safe and efficient retraction of the pipe followed by secondary jacking operations presents a significant engineering challenge.

(4) JPCCP consists of a heavy-duty, five-layer laminated composite pipe. The stability of the circumferential drag-reducing grout sheath is critical for ensuring smooth jacking through collapsible loess strata, and the selection of grouting material and the grouting process significantly influence both jacking efficiency and the pipe–soil interaction.

3. Key Design and Construction Techniques

3.1. Organization Design of Project

The project exhibits distinct characteristics, including stringent environmental protection requirements, intricate organizational challenges, and a compressed construction schedule. Table 3 shows the allocation of the overall construction tasks, highlighting that 15 caissons and 30 jacking intervals demand the highest allocation of resources, encompassing labor force, engineering materials, and construction machinery. Consequently, the project was compartmentalized into 5 distinct work areas, with 7 construction teams, utilizing a total of 14 pipe-jacking machines, engaged in around-the-clock construction to guarantee timely project completion.

Table 3. Allocation of the overall construction tasks.

S/N	Demarcation	Construction Contents
1	Open caisson	Reinforcing steel reinforcement, formwork installation, and concrete pouring.
2	Pipe jacking	Pipe-jacking construction and pipe joint treatment.
3	Earthwork	Open caisson earthwork excavation, earthwork transportation, and backfilling.
4	Pipe connection	Pipeline connection in the caisson, valve installation, etc.
5	Greening and municipal rehabilitation	Restoration of damaged greening and municipal facilities along the line.

The 15 caissons exhibit an average inner diameter of 22.5 m, with an average shaft depth of 28.7 m, including 7 caissons exceeding a depth of 30 m. The construction initiation for all caissons occurred in December 2022, concluding on 5 June 2023, spanning 178 days. Figure 4 illustrates the construction efficiency of caissons, with an average daily excavated earthwork volume of 83.8 m^3/d and a maximum daily excavated volume reaching 157.5 m^3/d. The 5# (L3) shaft boasted the largest internal diameter among the 15 caissons, measuring 34 m, but it exhibited the highest excavation efficiency, attributed to its broader site and more favorable geological conditions in the surrounding area.

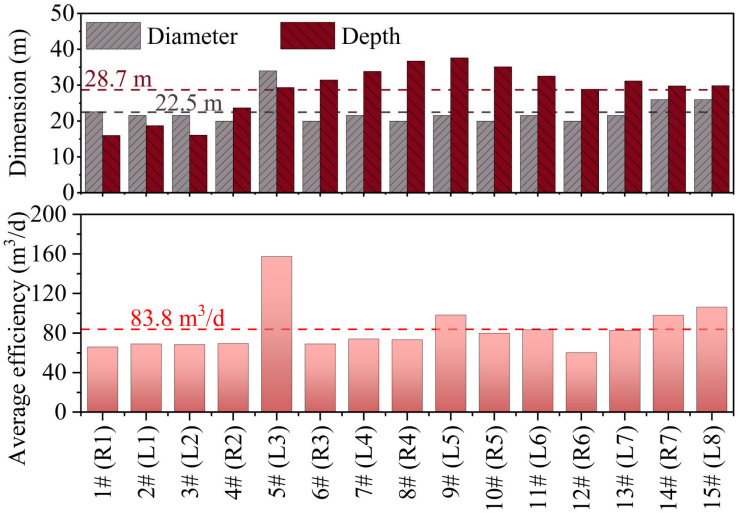
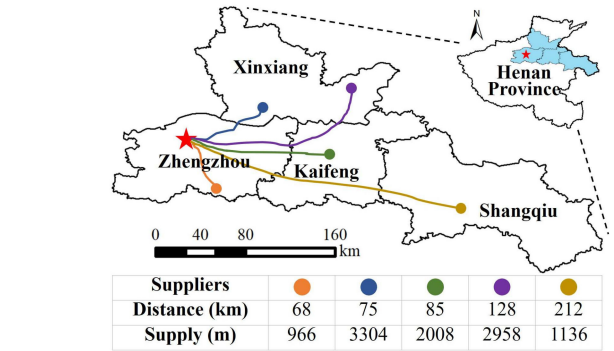


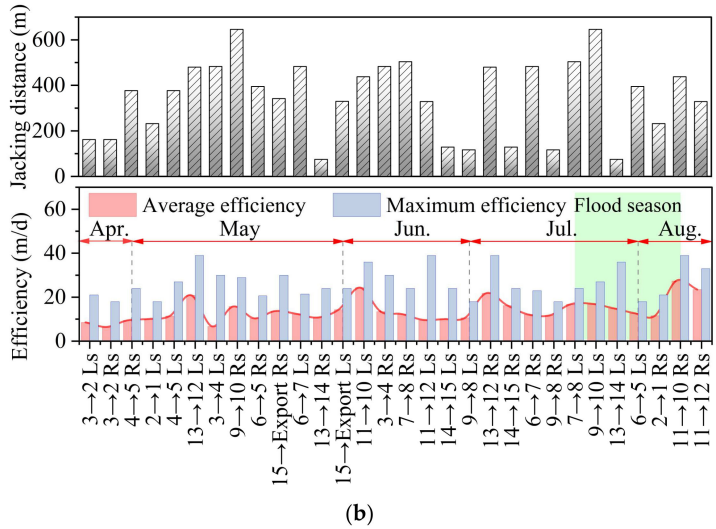
Figure 4. Comparison of open caissons excavation efficiency.

A total of 42 sets of production molds were utilized by 5 pipe suppliers for prefabricating JPCCPs, and the pipes were transported to the site after the production inspection. The construction organization design of the jacking pipes is depicted in Figure 5, with Figure 5a showing the location of 5 pipe suppliers relative to the construction area. Each supplier is

situated approximately 68~212 km away from the construction area, with supply distances ranging from approximately 966 to 3304 m, and this arrangement ensures the timely and sufficient availability of over 3600 pipes throughout the construction period.



(**a**)



(**b**)

Figure 5. Construction organization design of the pipe jacking: (**a**) suppliers' distribution and transportation route; (**b**) comparison of jacking efficiency.

Figure 5b illustrates the comparison of jacking efficiency for the 30 jacking intervals. Commencing with the initiation of the first jacking interval (3→2 L) on 2 April 2023, and concluding with the final jacking interval (9→10 R) on 31 August 2023, the completion of all tasks required 152 days, involving a peak of 11 concurrently operating pipe-jacking machines. The daily average work efficiency for the 3→2 jacking interval ranged from the minimum of 6.5 to 8.5 m/d, while the 11→10 jacking interval achieved a remarkable 36–39 m/d as the highest single-day efficiency. Over time, the average work efficiency consistently improved each month, and the flood season had little effect on the efficiency.

3.2. Design and Production of JPCCP

3.2.1. JPCCP Design

JPCCP, a new type of composite pipe fabricated from prestressed and non-prestressed reinforced concrete, exhibits a capacity to withstand the combined forces of external pressure incurred during jacking and internal water pressure during subsequent operation and maintenance. Notably, the project involves pipe jacking with a 4.8 m outer diameter, a longest single jacking interval of 646 m, a maximum burial depth of 40 m, and traverses collapsible loess stratum. Consequently, the pipe design must address issues encompassing structural stability, pipeline settlement uniformity, and effective sealing and waterproofing of bell-and-spigot joints.

Figure 6 illustrates the schematic structure of JPCCP, while Table 4 shows the primary structure and raw material parameters of JPCCP. To bolster the joints' strength, a 150 mm × 10 mm guard steel ring is affixed to the outer wall, while a 20 mm wooden pressure ring is secured to the spigot end face to mitigate excessive jacking force. Each ring is equipped with 4 positioned grouting holes at 90° intervals, interconnected by branch pipes featuring triple and straight valves. Symmetrically arranged at 180°, 2 pressure test holes are positioned in the middle of the two rubber rings of the spigot steel ring and sealed using M10 bolts.

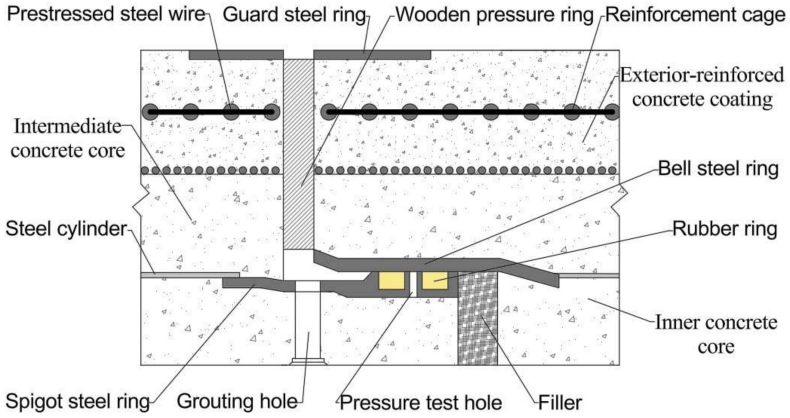


Figure 6. Schematic structure of JPCCP.

Table 4. The primary structure and raw material parameters of JPCCP.

Structure	Dimension	Performance Requirements
Bell steel ring Spigot steel ring Guard steel ring	236 mm × 10 mm 240 mm × 21 mm 150 mm × 10 mm	The minimum yield strength is not less than 235 MPa [4,5]
Steel cylinder	1.5 mm (THK)	The minimum yield strength is not less than 215 MPa [4,5]
Prestressed wire	7 mm (OD)	The tensile strength is 1570 MPa, and the control stress is 70% [4,5]
Reinforcement cage	12 mm (OD)	HRB400
Exterior-reinforced concrete coating	80 mm (THK)	C60
Intermediate concrete core	230 mm (THK)	C60
Inner concrete core	90 mm (THK)	C60

3.2.2. JPCCP Production

The spigot rings and bell rings are crafted from section steel, while the steel cylinder is formed through the welding of fixed-length thin steel plates or thin steel plate coils. The hydrostatic pressure test for the steel cylinder must endure a minimum duration of 3 min, and the height of the repair weld for any welding defects should not exceed 2.0 mm. In the vertical forming process of the concrete core, the vibration frequency and duration must be calibrated to ensure adequate compactness. According to GB19685-2017 [4] and SL 702-2015 [5], the concrete core undergoes two curing phases; following the conclusion of the initial steam curing and demolding, the cubic strength should not dip below 20 MPa. Before wire wrapping, the cubic strength of the concrete core should be at least 70% of the 28-day compressive strength and the initial compressive stress of the wire should not surpass 55% of the compressive strength. Throughout the wire winding process, automatic tension recorders should record any alterations in pre-tension. The reinforcement cage is

formed through roll welding, subsequently welded to the guard steel ring, and positioned at half the thickness of the cover concrete. Subsequently, the fabricated reinforcement cage undergoes secondary casting and steam curing.

After forming, the completed products are transported for outdoor curing via railcar. Repair for any cracks that may emerge on the internal surface of JPCCP involves the application of either cement slurry or epoxy resin, complemented by the use of an ultra-thick film of heavy epoxy coal tar as the external anti-corrosion coating. Post 28 days of curing, the spigot end face is affixed with a 20 mm wooden pressure transfer ring and the pipes are vertically transported by vehicles to the construction or stacking area. On the construction site, pipe turnover machines flip the vertical pipes, which are subsequently hoisted to the shaft's bottom by crawler cranes, initiating the jacking process for JPCCP. The process of manufacturing, transportation, and utilization of JPCCP are visually elucidated in Figure 7.

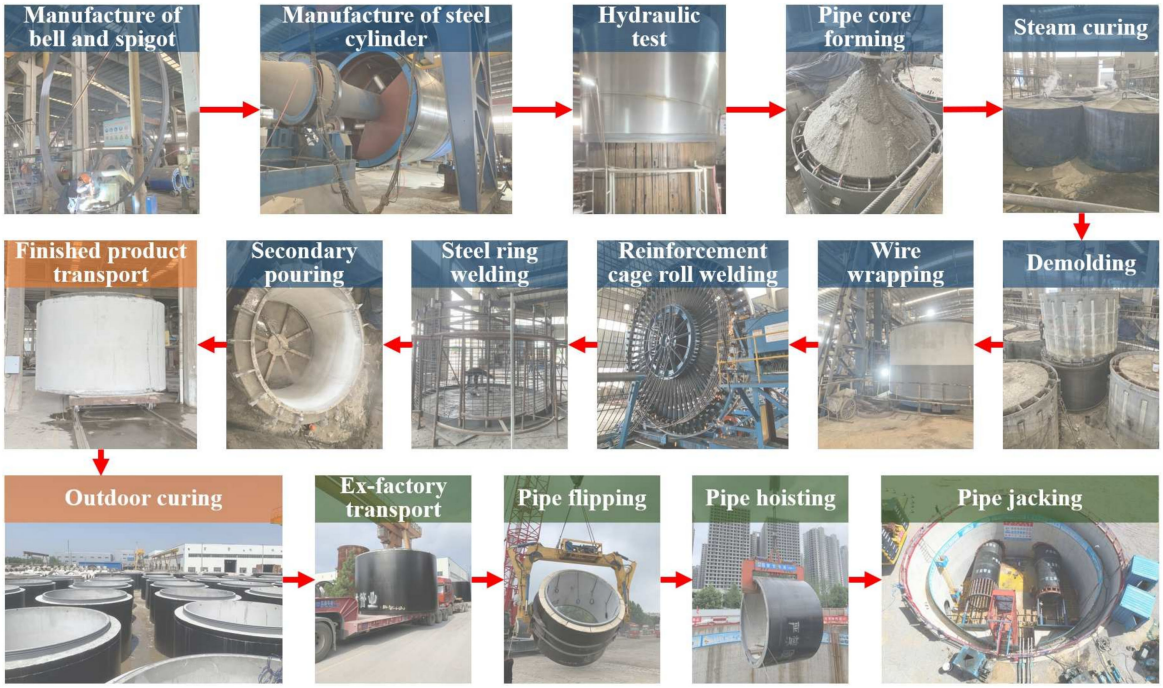


Figure 7. The process of manufacturing, transportation, and utilization of JPCCP.

3.3. Key Jacking Techniques of JPCCP

3.3.1. Selection of Pipe-Jacking Machine

A total of 14 slurry balance pipe-jacking machines were put into the project. In consideration of stratum characteristics, the tool combination of the center cutter, shell cutter, straight scraper, and side cutter on the cutterhead provides the cutterhead with obstacle-breaking capabilities. The cutterhead openings of the pipe-jacking machine across the 30 jacking intervals varied between 10% and 13%, with an opening size of 7 cm × 7 cm. Figure 8 shows the cutter arrangement of the pipe-jacking machine for the 3→2 jacking interval.

The cutterhead is prone to the occurrence of 'mud cake', particularly when the pipe-jacking machine crosses through the light silty loam-like loess or medium silty loam-like loess. The presence of 'mud cake' not only hinders the cutterhead's cutting efficiency but also impedes the jacking speed; hence, the design of the slurry circulation system must account for both the cutterhead and the slurry cabin. Effective prevention of cutting and slag discharge issues in the cutterhead across various layers—clay, sand, pebble, and rock—can be achieved by regulating the front, rear, and external water supply systems. Simultaneously, to prevent the 'mud cake' phenomenon, the opening features a central large

slag inlet, complemented by five flush outlets strategically arranged on the cutterhead's surface to enhance the plasticity of the muck. The key parameters of the pipe-jacking machines are comprehensively detailed in Table 5.

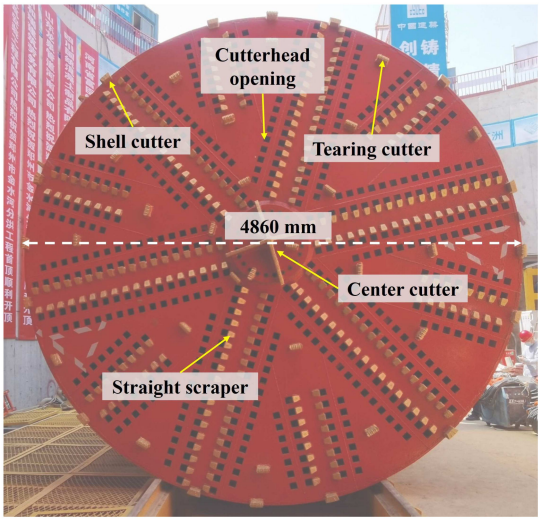


Figure 8. The cutter arrangement of the pipe-jacking machine for the 3→2 jacking interval.

Table 5. The key parameters of pipe-jacking machines.

Item	Technical Parameter	Value
Specification and dimension	Outside diameter of machine shell (mm)	4800
	Outside diameter of cutterhead (mm)	4860
	Length of pipe-jacking machine (mm)	4825
	Weight of machine head (t)	80
Cutterhead drive	Speed of cutterhead ($r \cdot min^{-1}$)	0~4.5
	Cutting disc cutting power (kW)	6 × 37
	Cutting torque of cutterhead ($kN \cdot m^{-1}$)	1600
	Cutterhead cutting coefficient ($kN \cdot m^{-2}$)	22.2
	Cutterhead opening rate	10%~13%
	Maximum permissible propulsion speed ($mm \cdot min^{-1}$)	50
Deflection-correcting system	Up-down deflection angle (°)	±3
	Left-right deflection angle (°)	±3
	Number of rectify cylinders	8
	Jacking force of single rectify cylinder (t)	200
	Jacking force of rectify cylinders (t)	2400

3.3.2. Jacking Process of JPCCP

The layout of the main equipment and devices at the launch shaft is depicted in Figure 9. At the position of the shaft opening, the steel sleeve and flange plate are pre-buried, and after the extension of the opening, sealing collars are installed in the front wall. Additionally, a water-stop curtain utilizes two annular rubber plates and intermediate support steel rings, with polyurethane poured into the center. Within the shaft wall and the main hydraulic cylinder frame, the reaction wall is established by combining the steel cushion box and reinforced wall, providing a vertical stress surface to bear the reaction force generated during pipe jacking, facilitated by the 20 mm-thick steel plate cushion iron. The primary jack cylinder opts for 8 to 10 single jacks, each capable of withstanding a force of 2000 kN, symmetrically arranged and affixed to the reaction wall.

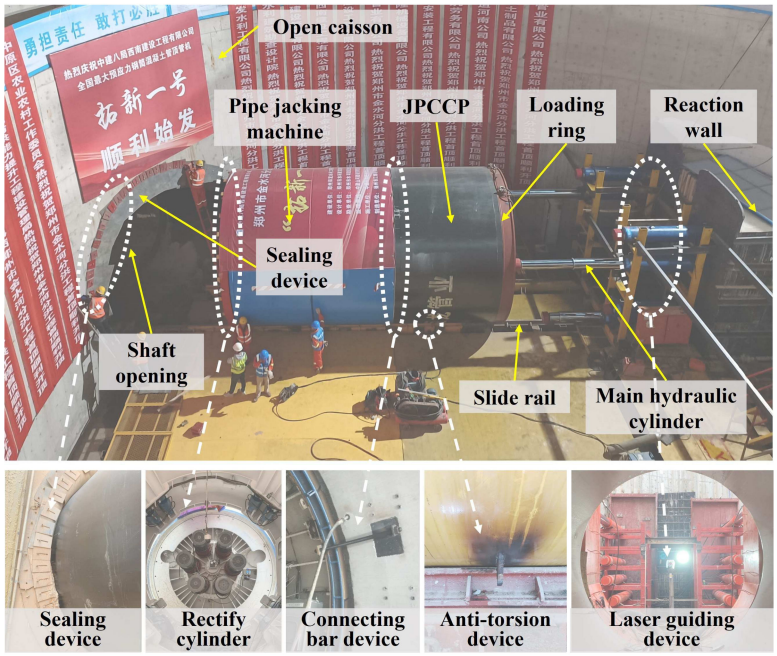


Figure 9. Layout of the main equipment and devices at the launch shaft.

At the initiation of pipe jacking, anti-torsion devices (20 mm-thick steel plates) are welded on both sides of the guide rail, at intervals of approximately 1.5 m, onto the rear cabinet of the machine; meanwhile, it is imperative to promptly cut and polish the anti-torsion devices to prevent any potential damage to the sealing device. The pipe-jacking machine, in conjunction with the initial 3 to 5 pipes, is seamlessly integrated through a connecting bar device, providing adequate anti-torsion reaction force. During the jacking process, alternating the left and right rotation of the cutterhead minimizes the unidirectional rotation time, thereby achieving an effective anti-torsion effect. In the phase of pipe connection, the jacked pipes are prone to being pushed back by active earth pressure. This issue can be addressed by welding a triangular reaction frame on either side of the machine or the subsequent pipe and incorporating transverse I-beams to support the pipe end, thus achieving the anti-retreat function.

During the jacking process, the clinometer in the front shell gauges horizontal attitude, elevation status, and deflection of the front shell; then, the rectify cylinder is employed to adjust the machine head's direction. The slurry pump, intake pump, and grouting pump are equipped with a frequency conversion system, enabling more effective adjustments to the jacking speed and flow rate. This system proves particularly effective in controlling the pressure within the slurry cabin, adapting to the various geological and soil conditions. To supply the electricity within the pipe, a 630 kVA electricity box is positioned at the entrance, with an additional power-supply cabinet situated within the pipe near the machine head. A mobile air compressor with a capacity of 6 m^3 is furnished with a φ50 ventilation duct to facilitate press-in ventilation; moreover, the rear shell of the machine head is outfitted with oxygen and carbon monoxide detectors to ensure a safe working environment.

During the receiving process, the position and elevation of the receiving frame align with the orientation of the pipe-jacking machine near the shaft opening. The elevation is intentionally set slightly lower than that of the machine, and a longitudinal slope is established to prevent the front-end sinking of the machine head. The sealing of the shaft door is achieved through the use of either a brick wall or concrete, while the inner side of the shaft opening is reinforced and supported by placed I-beams. Upon the machine's entrance into the shaft opening, the I-beams are initially removed, followed by the subsequent removal of the outer brick and reserved concrete. To ensure precision, the orientation of

the pipe-jacking machine undergoes manual assessment and measurement at intervals of 200 m, 100 m, and 50 m from the receiving shaft opening. Subsequently, a recheck measurement is performed to make necessary adjustments to the machine head upon reaching the shaft opening. The machine swiftly penetrates the shaft opening, and it is subsequently sealed using asbestos cement and C20 micro-expansion concrete.

3.3.3. Lubrication and Resistance-Reduction Technology

In pipe-jacking engineering, lubricating slurry is commonly employed to diminish the friction coefficient between the pipe wall and the surrounding soil, thereby minimizing resistance [17–19]. In this project, the resistance-reduction grouting process surrounding the pipe is categorized into synchronous grouting and replenishment grouting, each facilitated by independent pipelines, as illustrated in Figure 10. The grouting pump within the pipe directs the slurry to the grouting branch pipes of each grouting section through the grouting trunk pipe, with each pipe being equipped with a designated grouting section. Pressure gauges are strategically positioned at the leading edge of both the grouting pump and the grouting trunk pipe to regulate and fine-tune the grouting pressure. The lubricant slurry employed in the field is formulated with Na-bentonite, NaOH, carboxymethylcellulose (CMC), and water, and the proportion of Na-bentonite and water is 10% and 90%, respectively. Post configuration of the slurry, an aqueous solution incorporating PH-PAM-11/800 (Henan Anteng Mining Co. Ltd., Shangqiu, China) is introduced, suitable for grouting following thorough mixing and a standing time exceeding 24 h.

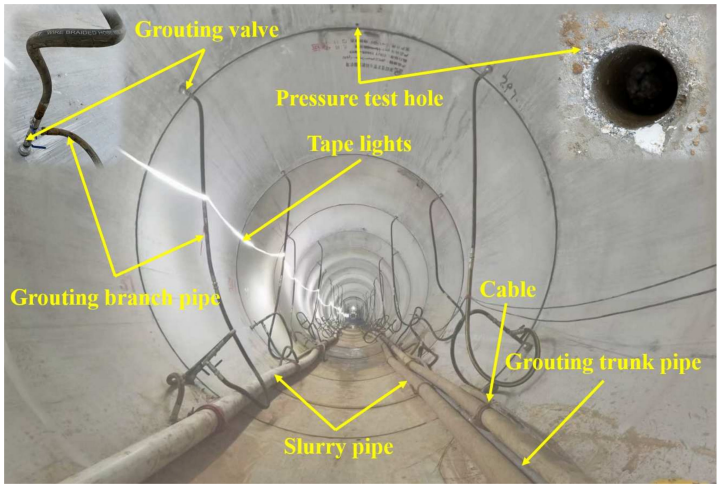


Figure 10. Layout of grouting section.

Considering the 7→8 L jacking interval as an illustrative case, the depth of the interval is approximately 34 m, with a length of 504 m and an average depth of about 33.8 m. This interval predominantly crosses through ② Light silty loam-like loess, as depicted in Figure 11, illustrating the variation curve of jacking force and friction resistance per unit area. In this jacking interval, the jacking force exhibits a generally smooth variation, consistently staying below 15,000 kN for the majority of the duration. In the initial 10 m, the pipe jacking primarily crosses through high-pressure rotating piles, characterized by a slow jacking speed and minimal control over jacking force, and the friction resistance per unit area of the pipe jacking is significant due to the non-utilization of the lubricant slurry. When jacked into the stratum, the jacking force continues to rise, accompanied by a sharp decline in friction resistance per unit area attributed to the application of the slurry. Despite intermittent fluctuations in the jacking force, the maximum fluctuation range remains below 3000 kN for a considerable period. The friction resistance per unit area around the pipe diminishes to less than 3 kPa once construction stabilizes (the distance exceeds 100 m),

and the unit friction resistance stabilizes at approximately 1.2 kPa in the later stages, which means that the slurry has achieved a good effect of resistance reduction [18].

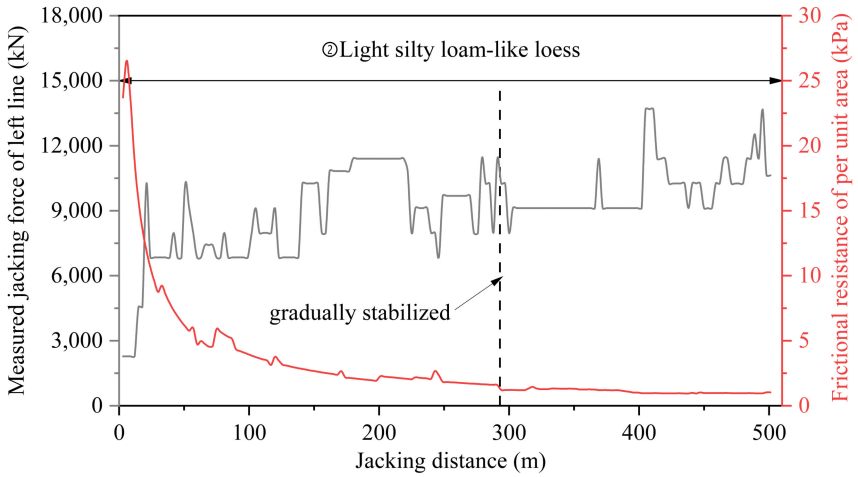


Figure 11. Variation curve of jacking force and friction resistance per unit area of the 7→8 L jacking interval.

3.4. Engineering Problems Countermeasures

The 14 pipe-jacking machine heads exhibit an average weight of 80 tons, and the heavier ones are susceptible to sinking, particularly when the soil adjacent to the shaft opening comprises a soft sandy layer. Notably, during the construction of the 11→12 L jacking interval, the front end sinking of the machine head occurred during the night stoppage following the jacking of 13 JPCCPs (approximately 39 m). Owing to the machine head being rigidly connected with the subsequent pipes via connecting bar devices, the entire pipeline is inclined downward.

A supplementary exploration of the site revealed that the pipe-jacking machine was located positioned in a silty sand stratum at this time, which was inconsistent with the old geological survey report. Based on the geological data obtained from the supplementary exploration, a remedial scheme for the pipe pullback and re-jacking of the jacking part was devised. The schematic diagram illustrating the front end sinking of the machine head and the pipe pullback is presented in Figure 12. The primary construction process of the pipe pullback involves the following: (1) removing the equipment in the pipes or machine head; (2) installing the pipe pullback steel strand; (3) arranging the reverse jack and T-shaped beam in the working shaft; (4) anchoring and straightening the reverse jack; (5) initiating the reverse jack to push the T-shaped beam and pull the steel strand back; (6) withdrawing the pipe incrementally.

Before and after the pipe pullback procedure, high-pressure rotary piles were employed to reinforce the soil near the opening and over the jacked distances. The pile spacing was set at 0.5 m, with a diameter of 110 mm, and the bottom elevation of the holes was controlled to be 10 cm above the jacking pipe. The reinforcement material consisted of a mixture of cement, water, and soil at a ratio of 1:2.5:8, and the compressive strength was verified on-site to be approximately 3 MPa after 7 days of curing. During the pullback process, grouting was first carried out using the existing grout pipes of the jacking machine and the ground boreholes with a grout pump. After an initial extraction of 50 cm, the outward pulling was paused to inspect the grouting situation and perform supplementary grouting. Approximately 10 m^3 of grout was injected during each cycle. Finally, the secondary jacking of JPCCP was executed after sealing the shaft opening with steel sheet piles and installing sealing collars.

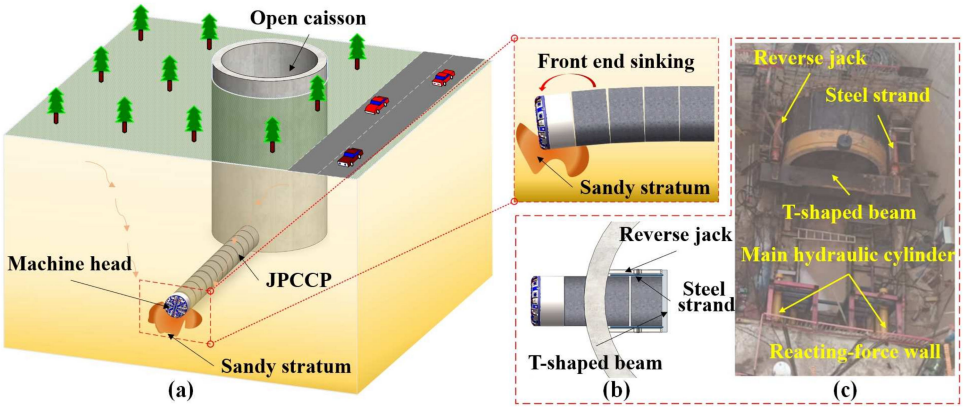


Figure 12. Schematic diagram of the front end sinking of machine head and the pipe pullback: (**a**) front end sinking of machine head; (**b**) pipe pullback; (**c**) photo of the scene.

4. Field Monitoring and Analysis

4.1. Monitoring Scheme

To investigate the variation of pipe–soil contact pressure in the jacking process of ultra-large diameter JPCCP within the collapsible loess stratum, a test pipe located in the 7→8 L interval was selected to monitor the contact and slurry pressure during the jacking operation. The total length of the 7→8 L interval is 504.5 m, with an average burial depth of 34 m. The test pipe selected for this study is Pipe No. 48 within the 7→8 L interval, located approximately 145.8 m from the preceding cutterhead. Monitoring commenced upon the pipe's installation at the launch shaft and continued until the completion of the jacking process. The total duration of the test was 22 days.

The experiment used earth pressure cells and pore water pressure gauges with high sensitivity, precision, and stability to continuously monitor the external contact pressure and slurry pressure in real-time. Figure 13 shows the arrangement diagram of pressure monitoring points around the No.48 pipe, with monitoring points positioned at the pipe's top, bottom, left, and right sides. As all sensors were of the vibrating-wire type, an MCU32 automatic data acquisition system was employed for data collection at a frequency of once every 20 min.

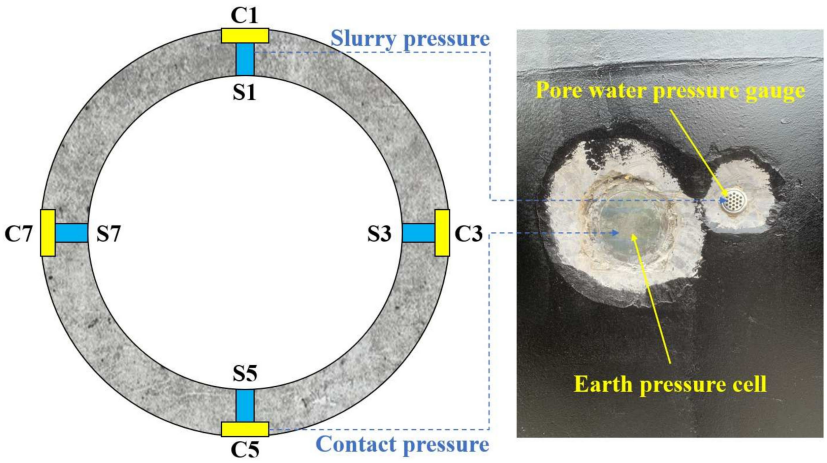


Figure 13. Arrangement diagram of pressure monitoring points around No. 48 pipe.

4.2. Monitoring Results

Figure 14 illustrates the variation curves of pressure around the test pipe during the jacking cycle, with Figure 14a depicting the contact pressure and Figure 14b depicting the slurry pressure. Due to the absence of slurry pressure data before August 3, the

corresponding data are omitted from Figure 14b. The figure reveals that the variation in pipe–earth pressure during the jacking of the test pipe can be categorized into three distinct phases:

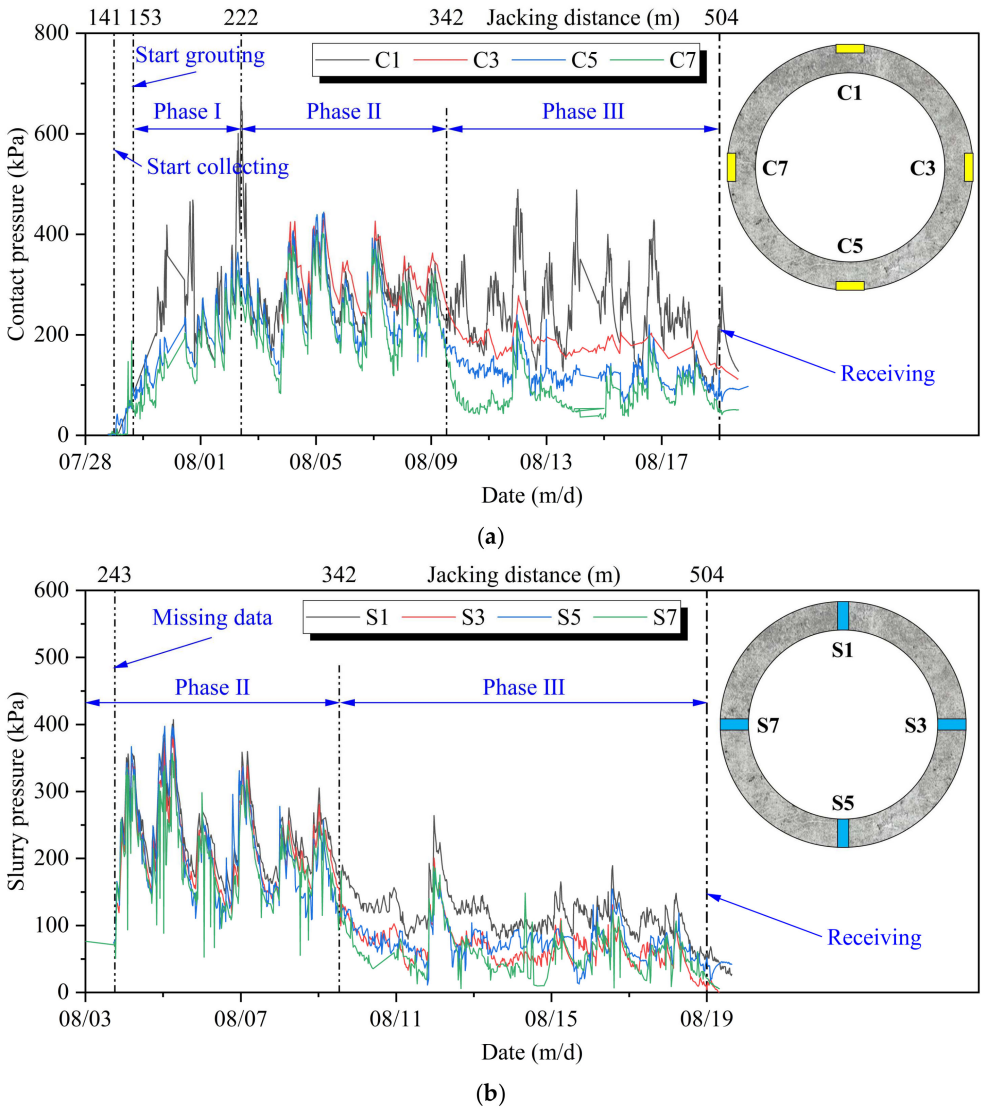


Figure 14. Variation curves of pressure around the test pipe: (**a**) contact pressure; (**b**) slurry pressure.

Phase 1: The pipe contact pressure increases steadily from zero as the pipe jacks approximately 80 m into the soil from the launch shaft.

Phase 2: Both the contact pressure and slurry pressure display sawtooth fluctuations, with the variation trends largely synchronized. During this phase, the slurry pressure remains between 100 kPa and 40 kPa, and the slurry pressure trends across all monitoring points are consistent. The grouting and grout replenishment frequency is relatively high, with excessive grouting or high grout pressure leading to significant fluctuations in the pipe–earth pressure.

Phase 3: Both the contact pressure and slurry pressure decrease, with slight differences in their variation trends. During this phase, the frequency of grouting and grout replenishment decreases, and the slurry pressure fluctuates within the range of 0 kPa to 250 kPa, with minor variations in slurry pressure values across different monitoring points. The slurry pressure stabilizes, exhibiting small fluctuations.

After the pipe has been received, although the slurry pressure does not fully dissipate, it typically remains between 0 kPa and 50 kPa. The slurry in the over-excavated annular

gap gradually dissipates, while the water pressure in the surrounding soil progressively exerts influence on the pipe.

As observed in Figure 14, the contact pressure and slurry pressure exhibit a similar variation trend to some extent during the jacking process, suggesting that the pipe contact pressure is predominantly governed by the grouting pressure. Feng Xin et al. [12] suggests that the difference between the contact pressure and the slurry pressure can be interpreted as the effective earth pressure exerted on the pipe, with a value of 0 indicating complete stability of the bore wall and no interaction between the pipe and the surrounding soil. As illustrated in Figure 15, the effective earth pressure curves for each monitoring point on the test pipe are presented. The average effective earth pressures at the right side and bottom of the pipe are 109 kPa and 50 kPa, respectively, with relatively stable fluctuations. In contrast, the effective earth pressures at the top and right sides of the pipe show substantial fluctuations. The primary cause of this phenomenon is that the pipe makes contact with the soil at 0° and 90° orientations, with variations in earth pressure leading to fluctuations in the contact pressure. Furthermore, factors such as pipe deflection during construction may increase localized additional contact pressure.

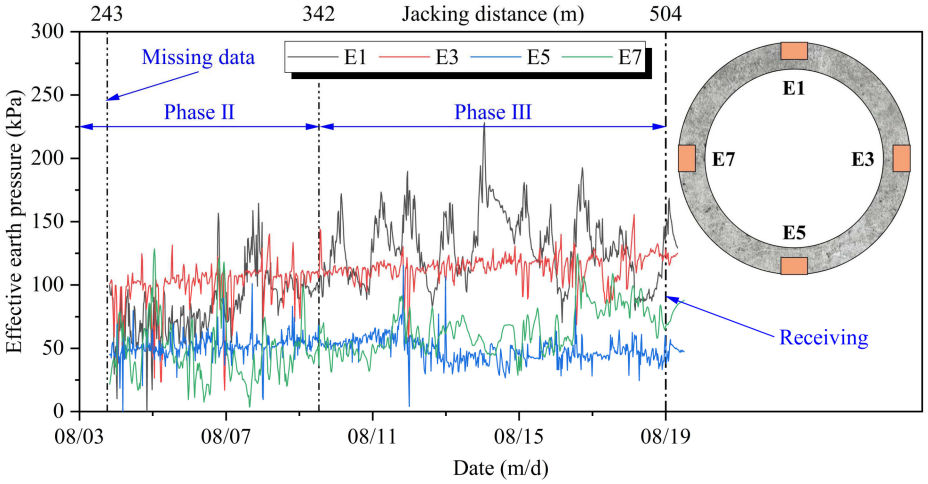


Figure 15. Variation curves of effective earth pressure around the test pipe.

4.3. Discussion

4.3.1. Pipe–Soil–Slurry Interaction

The pipe–soil–slurry interaction is a crucial concept that characterizes the interaction between the pipe and the surrounding soil, directly influencing the distribution of pipe loads and serving as a theoretical foundation for mechanical analysis during the jacking process [20]. From the perspective of pipe–soil contact characteristics, Figures 14 and 15 illustrate that in Phase II, the contact pressure is predominantly governed by the slurry pressure, with only minor fluctuations in effective earth pressure. In contrast, in Phase III, where the slurry pressure is relatively low, the slurry pressure stabilizes and the effective earth pressure exhibits considerable fluctuations, with the pipe–soil–slurry contact state undergoing frequent changes. Through analysis of the effective earth pressure at each monitoring point, it was observed that in Phase II, the maximum effective earth pressure occurs at the E3 (90°) point, indicating that the pipe tends to make direct contact with the soil on the right side. In Phase III, the effective earth pressures at the E1 (0°) and E3 (90°) points are comparatively high, causing the pipe–soil contact orientation to shift towards the upper right side of the pipe. Figure 16 depicts the two potential pipe–soil–slurry interaction states during the two phases.

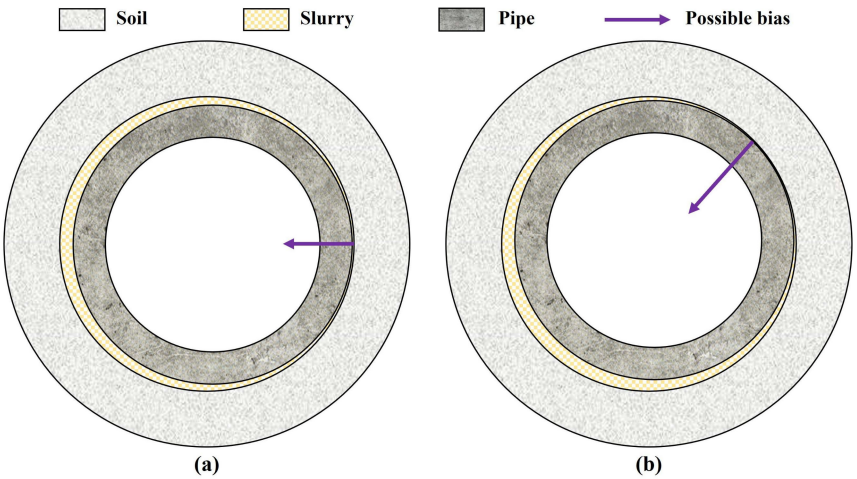


Figure 16. Pipe–soil–slurry interaction in different stages: (**a**) Phase II; (**b**) Phase III.

4.3.2. Calculation of the Earth Pressure

In general, when the buried depth (C) above the pipe is greater than or equal to twice the pipe diameter (D), the pipe-jacking project is typically classified as deep-buried pipe jacking. From the perspective of shear zone failure, deep-buried pipe jacking refers specifically to a scenario where the shear zone does not propagate to the surface during the pipe-jacking construction process. Existing studies suggest that the vertical earth pressure for deep-buried pipe jacking is typically calculated based on the Terzaghi theory [21], with the Terzaghi formula presented in Equation (1):

$$\sigma_z = \frac{1 - e^{-2K\tan\delta\frac{Z}{B_e}}}{2K\tan\varphi}(\gamma B_e - 2c) + qe^{-2K\tan\delta\frac{Z}{B_e}} \quad (1)$$

where C denotes the buried depth above the pipe; γ denotes the soil unit weight; c denotes the soil cohesion; K denotes the earth pressure coefficient; δ denotes soil internal friction angle; B_e represents the width of the loosened zone width, corresponding to the pipe's influence width; and q denotes the surface load, where $q = \sigma_{z=0}$.

In practice, the Terzaghi theory is widely adopted internationally for calculating the overburden load on pipe, with Table 6 presenting the parameter values from the national standards of various countries [22]. While the fundamental calculation formulas in these standards are similar, discrepancies exist in the selection of parameters, especially concerning the soil's shear characteristics. The values for the internal friction angle and lateral pressure coefficient vary across different national standards, which could influence the earth pressure calculations in pipe-jacking projects.

Table 6. Main modified parameters for different Terzaghi arching models.

Norms/Theories \ Empirical Parameters	B_e	δ	K	c
Terzaghi [21]	$D_p(1 + 2\tan a)$	φ	1	c
GB 50332 (China) [23]	$D_p(1 + \tan a)$	$K\tan\varphi = 0.19$		0
CECS 246 (China) [24]	$D_p(1 + 2\tan a)$	$K\tan\varphi = 0.11$~0.165		c
JMTA (Japan) [25]	$(D_p + 0.08)(\sec a + \tan a)$	φ	1	c
PJA (Britain) [26]	$D_p(\sec a + \tan a)$	φ	$K_a = \tan^2 a$	0
ATV A161 (German) [27]	$3^{0.5}D_p$, $\varphi = 30°$	$\varphi/2$	$K_0 = 0.5$	0
ASCE 27 (America) [28]	D_b	$K\tan\varphi = 0.11$~0.19		c

Table 7 presents the fundamental calculation parameters for the stratum in which the test pipe is situated. These parameters were substituted into Equation (1) and the national standard formulas provided in Table 6 to calculate the overburden load, as illustrated in Figure 17. The loosened zone width according to the Terzaghi theory and CECS 246 is the largest, measuring 11.8 m, while ASCE 27 restricts it to 4.9 m. Regarding earth pressure calculations, the PJA provides a maximum value of 362.7 kPa, while ASCE 27 specifies a minimum value of only 108.6 kPa. A comparison shows that the effective earth pressure at the top of the pipe in Phase II remains relatively stable, ranging from 50 to 100 kPa, while in Phase III, it stabilizes within the range of 100 to 180 kPa. At this phase, the overburden pressure on the pipe is more closely aligned with the calculated results from ATV A161 and ASCE 27.

Table 7. Basic calculation parameters.

Basic Parameter	Pipe Diameter	Buried Depth	Internal Friction Angle	Density	Coefficient of Earth Pressure at Rest	Coefficient of Active Earth Pressure
	D_p (m)	C (m)	φ (°)	ρ (g/cm^3)	K_0	K_a
Value	4.8	32	17.8	1.91	0.69	0.53

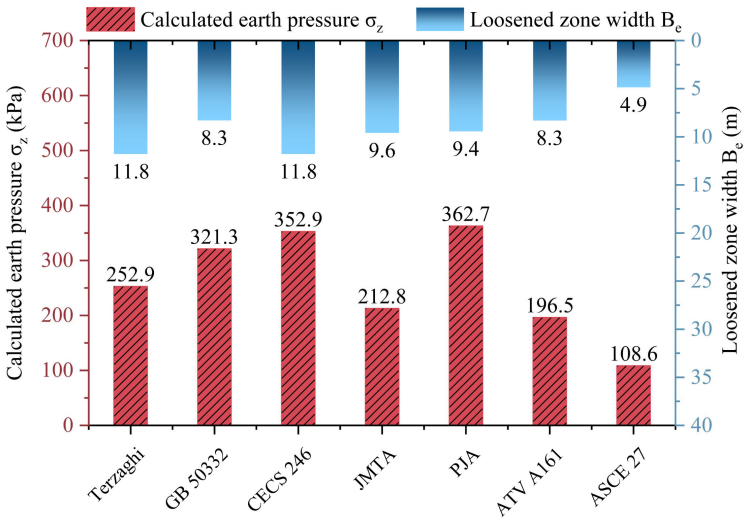


Figure 17. Earth pressure calculated by national standards of various countries.

5. Conclusions

This paper presents a case study of a significant flood diversion pipe-jacking project that crosses through the collapsible loess stratum in China and summarizes the technologies utilized in designing, constructing, and monitoring technologies associated with large-diameter JPCCP. Building upon this foundation, the study investigates strategies for addressing the engineering challenges encountered and explores the field testing methodologies for monitoring pressure surrounding pipes. The main conclusions are outlined as follows:

(1) Through the planning of the organizational design of the construction process and the optimization of supply routes, the pipeline was successfully and efficiently implemented within the designated construction period. The open caisson achieves a maximum excavation efficiency of 157.5 m^3/d, while pipe jacking attains 39 m/d.

(2) A systematic overview of the design and production processes of ultra-large-diameter JPCCP is provided. Through the strategic design of cutterhead opening ratios and tool

combinations; improvements to the double-row slag inlet design; and optimization of the front, rear, and external water supply systems, the formation of "mud cake" on the cutterhead is effectively mitigated, thereby ensuring the efficiency and reliability of the pipe-jacking process.

(3) The on-site grouting system employs a slurry pump, intake pump, and grouting pump with a variable-frequency drive, effectively regulating slurry pressure and jacking speed while simultaneously reducing the frictional resistance per unit area of the large-diameter pipe. In response to the incident involving the front-end sinking of the machine head, a reverse pull-back method coupled with high-pressure rotary jet grouting pile techniques was employed, thereby ensuring the smooth progression of the jacking operation after the secondary jacking.

(4) Pipe–soil contact pressure monitoring tests on the pipe revealed that the contact pressure closely mirrors the fluctuations in slurry pressure. During jacking, pressure can be categorized into three distinct phases based on grouting frequency or pressure. Following pipe receipt, slurry pressure gradually diminishes, while water pressure increases, applying force on the pipe. The effective earth pressure, defined as the differential between contact pressure and slurry pressure, serves as a more reliable indicator of the pipe–soil–slurry contact state.

(5) During Phase II, the pipeline experiences relatively minimal fluctuations in effective earth pressure, predominantly in direct contact with the soil on the right side. In Phase III, significant fluctuations in effective earth pressure occur, and the pipe–soil–slurry contact state undergoes frequent transitions. A comparative analysis of calculation results from various standards reveals that the effective earth pressure at the pipe top is more consistent with the values derived by ATV A161 and ASCE 27.

Author Contributions: Conceptualization, H.Z.; methodology, H.Z. and S.H.; formal analysis, H.Z.; data curation, P.M.; investigation, H.Z. and H.W.; resources, H.W. and B.M.; funding acquisition, B.M. and P.M.; writing—original draft, H.Z. and S.H.; writing—review and editing, H.Z. and S.H. All authors have read and agreed to the published version of the manuscript.

Funding: This study was supported by the National Natural Science Foundation (NSFC No.52208410) of China, the Department of Science and Technology of Guangdong Province (2021ZT09G087), and the Guangzhou major science and technology special projects (20220602JBGS01).

Data Availability Statement: The data presented in this study are available on request from the corresponding author.

Acknowledgments: The authors are grateful to Zhengzhou Zhengfa Water Conservancy Engineering Co., Ltd. and China Construction Eighth Engineering Division Corp., Ltd. Southwest for their cooperation in the field tests and data collection.

Conflicts of Interest: Author Haitao Wang was employed by the company Zhengzhou Zhengfa Water Conservancy Engineering Co., Ltd. The remaining authors declare that the research was conducted in the absence of any commercial or financial relationships that could be construed as potential conflicts of interest.

References

1. Wu, Y.; Yu, G.; Shao, Q. Resilience benefit assessment for multi-scale urban flood control programs. *J. Hydrol.* **2022**, *613*, 128349. [CrossRef]
2. Sterling, R.L. Developments and research directions in pipe jacking and microtunneling. *Undergr. Space* **2020**, *5*, 1–19. [CrossRef]
3. Zhang, X.; Shen, Y.; Fan, Y.; Gao, X. Experimental study on the triaxial compression mechanical performance of basalt fiber-reinforced recycled aggregate concrete after exposure to high temperature. *Case Stud. Constr. Mater.* **2024**, *20*, e03026. [CrossRef]
4. *GB/T 19685*; Prestressed Concrete Cylinder Pipe. China Standards Press: Beijing, China, 2017.
5. *SL702 2015*; Technical Specifications of Prestressed Concrete Cylinder Pipe. China Water and Power Press: Beijing, China, 2015.

6. Zhang, Y.; Yan, Z.-G.; Zhu, H.-H.; Ju, J.W. Experimental study on the structural behaviors of jacking prestressed concrete cylinder pipe. *Tunn. Undergr. Space Technol.* **2018**, *73*, 60–70. [CrossRef]
7. Shen, Y.; Ling, J.; Lu, X.; Zhang, Y.; Yan, Z. Steel wire prestress analysis of large section jacking prestressed concrete cylinder pipe (JPCCP): Site experiment and numerical investigation. *Thin-Walled Struct.* **2023**, *184*, 110420. [CrossRef]
8. Zhang, Y.; Yan, Z.-G.; Zhu, H.-H. A full-scale experimental study on the performance of jacking prestressed concrete cylinder pipe with misalignment angle. In *Proceedings of GeoShanghai 2018 International Conference: Multi-physics Processes in Soil Mechanics and Advances in Geotechnical Testing*; Springer: Berlin/Heidelberg, Germany, 2018; pp. 345–354.
9. Zhou, H.; Huang, S.; Ma, B.; Zhang, H.; Tan, X.; Zhao, Y.; Ma, P.; Su, X.; Wei, Y. Full-scale test study on the mechanical response of ultra-large section jacking prestressed concrete cylinder pipe (JPCCP) under axial jacking force. *Tunn. Undergr. Space Technol.* **2025**, *155*, 106194. [CrossRef]
10. Zhou, H.; Huang, S.; Ma, B.; Zhao, Y.; Tan, X.; Zhang, H. Prestressed steel wires impact on axial bearing capacity of ultra-large section jacking prestressed concrete cylinder pipe (JPCCP): Field experiment and simulation. *Eng. Fail. Anal.* **2025**, *167*, 109046. [CrossRef]
11. Khodabandeh, M.A.; Nagy, G.; Török, Á. Stabilization of collapsible soils with nanomaterials, fibers, polymers, industrial waste, and microbes: Current trends. *Constr. Build. Mater.* **2023**, *368*, 130463. [CrossRef]
12. Feng, X.; Zhang, P.; Chen, X.; Zhang, Y.; Ma, B.; Liu, K.; Xu, T.; Zeng, C. Field mechanical properties of large section concrete pipes during jacking in fractured moderately weathered siltstone. *Tunn. Undergr. Space Technol.* **2023**, *131*, 104818. [CrossRef]
13. Liu, W.; Tan, J.; Shi, J.; Huang, X.; Chen, W. A Method for calculating jacking force of parallel pipes considering Soil Arching Effect and Pipe-Slurry-Soil Interaction. *Comput. Geotech.* **2024**, *173*, 106528. [CrossRef]
14. Liu, S.; Zhang, B.; Wang, H.; Cheng, J.; Cai, C.; Wang, X.; Lv, C. Large-scale field test on the shear behavior of concrete pipe-silty soil interfaces in pipe jacking: A case study. *Constr. Build. Mater.* **2024**, *419*, 135470. [CrossRef]
15. Liu, Y.; Liu, W.; Lin, Y.; Zhang, X.; Zhou, J.; Wei, B.; Nie, G.; Gross, L. Urban waterlogging resilience assessment and postdisaster recovery monitoring using NPP-VIIRS nighttime light data: A case study of the 'July 20. 2021' heavy rainstorm in Zhengzhou City, China. *Int. J. Disaster Risk Reduct.* **2023**, *90*, 103649. [CrossRef]
16. *GB/T 50025*; Standard for Building Construction in Collapsible Loess Regions. China Standards Press: Beijing, China, 2018.
17. Shou, K.; Yen, J.; Liu, M. On the frictional property of lubricants and its impact on jacking force and soil–pipe interaction of pipe-jacking. *Tunn. Undergr. Space Technol.* **2010**, *25*, 469–477. [CrossRef]
18. McCabe, B.A.; O'Dwyer, K.G.; Sheil, B.B. Skin friction increases associated with pipe-jacking stoppages modelled using direct shear interface tests. *Tunn. Undergr. Space Technol.* **2025**, *156*, 106147. [CrossRef]
19. Ong, D.E.L.; Choo, C.S. Assessment of non-linear rock strength parameters for the estimation of pipe-jacking forces. Part 1. Direct shear testing and backanalysis. *Eng. Geol.* **2018**, *244*, 159–172. [CrossRef]
20. Vazouras, P.; Dakoulas, P.; Karamanos, S.A. Pipe–soil interaction and pipeline performance under strike–slip fault movements. *Soil Dyn. Earthq. Eng.* **2015**, *72*, 48–65. [CrossRef]
21. Terzaghi, K. *Theoretical Soil Mechanics*; John Wiley & Sons Inc.: Hoboken, NJ, USA, 1943; pp. 66–76.
22. Zhang, H.; Zhang, P.; Zhou, W.; Dong, S.; Ma, B. A new model to predict soil pressure acting on deep burial jacked pipes. *Tunn. Undergr. Space Technol.* **2016**, *60*, 183–196. [CrossRef]
23. *GB/T 50332*; Structural Design Code for Pipeline of Water Supply and Waste Water Engineering. China Standards Press: Beijing, China, 2002.
24. *CECS 246*; Technical Specification for Pipe Jacking of Water Supply and Sewerage Engineering. China Planning Publishing House: Beijing, China, 2008.
25. Japan Microtunnelling Association. *Microtunnelling Methods Serious II, Design, Construction Management and Rudiments*; Japan Microtunnelling Association: Tokyo, Japan, 2013; pp. 69–72.
26. Pipe Jacking Association. *Guide to Best Practice for The Installation of Pipe Jacks and Microtunnels*; Pipe Jacking Associatio: London, UK, 1995; pp. 47–48.
27. *ATV-A 161 E-90*; German ATV Rules and Standards. Structural Calculation of Driven Pipes. The German Association for Water, Wastewater and Waste: Hennef, Germany, 1990; pp. 18–20.
28. *ASCE 27-00*; Standard Practice for Direct Design of Precast Concrete Pipe for Jacking in Trenchless Construction. ASCE: Reston, VA, USA, 2001; pp. 8–9.

Disclaimer/Publisher's Note: The statements, opinions and data contained in all publications are solely those of the individual author(s) and contributor(s) and not of MDPI and/or the editor(s). MDPI and/or the editor(s) disclaim responsibility for any injury to people or property resulting from any ideas, methods, instructions or products referred to in the content.